

Diagenesis Severely Modified Reservoir Characteristics: A Unique Carbonate Reservoir from Alur Siwah Field, Indonesia*

Ricardo Maranu¹, Ismail Syarifuddin¹, Erham Adhitiawan¹, Nadia Nurul¹, Miftahurochman Miftahurochman¹, Ferry Baskaraputra¹, Luqman Luqman¹, Yudi Yanto¹, and Joan Lumban Tobing¹

Search and Discovery Article #20203 (2013)

Posted August 26, 2013

*Adapted from extended abstract prepared in conjunction with oral presentation at AAPG Annual Convention and Exhibition, Pittsburgh, Pennsylvania, May 19-22, 2013, AAPG©2013

¹MedcoEnergi, Jakarta, Indonesia (maranu.ricardo@gmail.com)

Abstract

Building a geological model of a Lower Miocene carbonate reservoir in South East Asia region frequently offers huge challenges in defining the depositional facies model and reservoir characterization. A dynamic depositional system combined with multiple sub-aerial exposures could give a certain degree of complication in reservoir properties, especially due to porosity modification and changes in permeability. Bioclastic limestone with various degrees of reservoir quality are described from core data with high inconsistencies of porosity and permeability values along with depth on the same lithofacies. Multilayered porosity development was found in some wells and confirmed by well test data that multiple sub-aerial exposure more likely occurred rather than a single sub-aerial exposure event. Integration of core data and petrophysical analysis in decoding this complexity into more definite rock types has been a key process in building the input for distributing the properties from cored section to un-cored section and eventually to areas between wells supported by seismic data. A new reprocessed 3D seismic dataset was used for structural and stratigraphic interpretation, including multi-attribute analysis and seismic inversion (AI) for reservoir property prediction. Five zones of conventional interpretation have been generated, bounding internal seismic characters of transgressive, prograding and aggrading units which suggest different layering methods and probabilistic approaches have to be applied for each different unit. Seismic inversion results show high porosity correlates with low acoustic impedance and low porosity is the opposite. Highest cross correlation (0.7) is calculated between actual and predicted effective porosity logs in the study area. The final AI model provides geologically more realistic predicted effective porosity distribution and helps in understanding the subsurface image. Advanced probabilistic approaches were applied on 3D static model integrates the depositional facies, diagenesis processes, petrophysical analysis, and seismic inversion. As a result an appropriate 3D geological model can be constructed for unique reservoir geology.

Introduction

The Alur Siwah Field is located onshore in Block A PSC, about 45 km southeast of the Arun Gas Field ([Figure 1](#)). The field was discovered in 1972 by Asamera Oil. The main reservoir is limestone of the Peutu Formation which is encountered at an approximate depth of -2900 m subsea. To date, ten wells have been drilled in order to delineate and test the Alur Siwah structure for gas production. Of these wells, only six wells proved a significant gas column for commercial development.

Alur Siwah-1 (AS-1) and AS-6 wells were drilled to the shallower target, the younger Seureula and Keutapang sands that became the main reservoirs in Julu Rayeu Field, which is a shallow structural closure overlapping the north end of Alur Siwah. AS-2 was drilled off-structure on the eastern flank of the Alur Siwah structure to search for the oil rim in this field, but the result was water-bearing Peutu limestone with gas shows. AS-2 recovered 18.3 meters of conventional core. The AS-3 discovery well was drilled near the crest of the structure. The well found 98 meters of net gas pay in a 392 meter buildup of Peutu Limestone. AS-4 was drilled to prove oil accumulation in the north-central part of Alur Siwah. This well encountered around 70 meters of Peutu Limestone. A total of 38.5 meters of Peutu limestone was recovered during the coring. No log data has been acquired from this well as the well blew out during coring operation. AS-5 then drilled on the western edge of this field and penetrated the Peutu at the gas water contact of - 2920 meters subsea. AS-7A (redrill of AS-7 due to problems with surface casing) was drilled near the field southern limit and it penetrated a massive 458 meters of Peutu limestone; there were 55 sidewall core samples taken.

AS-8 was drilled in the northern part of the field, about 2.5 km northwest of AS-4. It was designed to help define the extent and reserves of the Alur Siwah Gas Field, especially in the north-central part of the field. It penetrated 45 meters of Peutu limestone (all within the gas column) and underlying the Tampur Dolomite and there were 33 sidewall core samples taken from both formations. AS-9 was drilled about 400 m southwest and about 30 m structurally updip from the AS-3. It was drilled to a final depth -2900 meters subsea about 20 m above the GWC. Conventional cores and side wall cores were taken in this well; about 6.9 meters of Peutu limestone was recovered from conventional coring along with 58 side wall core samples. AS-10 was drilled in the north-central part of Alur Siwah ([Figure 2](#)), it was a replacement well for AS-4, located about 900 m southwest. This well recovered 13.9 meters of Peutu Limestone from conventional coring. Critical data from the Alur Siwah wells are: (1) wireline logs and DST, (2) a total of 77.6 m of conventional core and 146 side wall core samples, and (3) an onshore 3D seismic survey covering the discovered reservoir.

Geologic Setting

The Alur Siwah Field is located on the North-South Rayeu Hinge (platform) that is bordered to the north by Alur Rambong-Malacca shelf and south by the Barisan-Tangsaran anticlinorium. The west border is Lokop-Kutacane Fault zone which separates the Rayeu hinge from Lhok Sukon Deep and toward the east, the platform forms the flexural zone of Tamiang deep. Geologically, Alur Siwah is a favorable area for carbonate development and bounded by two deep areas with potential for source rock development bounded by two deep regions that provide good potential for hydrocarbon source rock development. Four way dip carbonate build up closure, incorporated with North-South and NE-SW trending faults, are clearly defined from seismic sections. The nearest and potential kitchen for Alur Siwah Field is Tamiang deep where the Bampo Shale develops and is considered to be mature source rock. Nevertheless, the Lhok Sukon deep also has potential to charge the Alur Siwah reservoir. Geochemical analysis of Bampo Shales shows high Total Organic Content (TOC) and Hydrogen Index. Kerogen type for this

source rock is type 2-3 which is considered as mix of oil and gas prone. Basin modeling and burial history suggest that the Bampo Formation has reached gas generation conditions in Block A area.

Stratigraphic Framework

The Tampur Formation is assigned to the Eocene sedimentary sequence and was deposited unconformably overlying the Pre-Tertiary basement consisting of massive recrystallized dolomite and limestone. It is probably part of the pre-rift sequence deposited before the initial rifting in the basin. A thick sequence of conglomerate, breccia and muddy sandstone called the Bruksah Formation unconformably overlies the Tampur and older rocks in some outcrops and wells around Block A. The Oligocene Bruksah Formation represents the syn-rift phase of the basin filling with detritus shed from uplifted areas of the north-south trending horst systems and the high standing Malacca Shelf. Bruksah deposits are restricted to paleo-lows or basinal areas. The Bruksah is overlain by the Bampo Formation consisting of limestone, black marine shale, siltstone and fine sandstone. Outcrop and subsurface samples indicate ages of Late Oligocene to Early Miocene, based on foraminifera, and indicate shallow to deep marine environments.

A quiescent period followed Bruksah and Bampo sedimentation. Shallow water carbonates of the Peutu Formation accumulated on high standing platforms, while calcareous shale, sandstone and shaly limestone of the Belumai Formation were deposited in lower areas. These formations represent the post-rift sediments. Paleontologic data indicate the age of the Peutu and Belumai formations is Early Miocene. The Peutu likely represents a cycle of high-stand carbonate accretion, whereas basinal Belumai clastics accumulated during intervening low-stands. Belumai deposits are absent on the Alur Siwah uplift, but seismic lines show a wedge of the Belumai expanding down-dip to the east of the structure. Peutu Limestone varies in thickness from 35 to 50 meters of platform deposits to between 300 to 460 meter buildups of coral reef and foraminifera banks. It represents the primary reservoir rock for gas accumulation in Block A, such as the Alur Siwah and Kuala Langsa fields

The transgressive period that occurred during Miocene resulted in the deposition of post-rift Early Miocene clastics of the Belumai Formation. The clastics were primarily derived from northwest and northeast. Meanwhile the horsts became submerged, which resulted in carbonate deposition associated with carbonate build-ups. As transgression continued, the area received deeper marine shale of the Baong Formation. The change from paralic environments in the Peutu Limestone to bathyal deposits of the overlying Baong Shale reflects a change in tectonic regime as well as a rise in relative sea level. The Middle Baong Sands were derived from the Malacca Platform to the northeast extending to the southwest to a shale-out line located between the Alur Rambong and Alur Siwah fields. Erosion of pre-existing structural highs resulted in a widespread unconformity within zone N14. Except for thin local sands above the unconformity, the overlying Upper Baong consists of clay-rich mudstone. Paleo-environment deepened again to bathyal depths, followed by gradual shoaling upward into paralic sands of the overlying Keutapang Formation. These sand beds prograded northeastward from source terrain in the rising Barisan Mountain.

Following the deposition of the Baong Formation, the Keutapang Formation marks the first major event of deltaic sedimentation in the central part of the basin. Lithology consists of sandstones and conglomerates inter-bedded with subordinate shales. The sandstones are commonly glauconitic and fossiliferous. Keutapang reservoirs contain most of the oil discovered in the North Sumatra Basin. The upper contact of the Keutapang is poorly defined in outcrop and subsurface: this boundary appears to be gradational. The overlying shaly sediments of the Seureula Formation have undergone weathering processes recessively to form low rounded hills. The Seureula Formation consists of bluish gray shale

inter-bedded with fine to coarse and locally conglomeratic sandstones. The Seureula, which is early Pliocene, belongs to zones N18 to N19 and varies in thickness from 700 to 900 meters.

The Late Pliocene Julu Rayeu Formation consists of coarse clastics. Thin lignite occurs in shales inter-bedded with Julu Rayeu sands with paleo- environment vary from alluvial to paralic. Unconformably overlying the Julu Rayeu are Pleistocene terrace deposits of gravel, silt and mud. Holocene pro-gradation of the Arakunda River has extended the modern coastal plain about 5 kilometers east of Pleistocene terraces at the Alur Rambong ([Figure 3](#)).

Depositional Facies and Environment

General observation of depositional facies of Alur Siwah reservoir demonstrates a predominantly muddy facies reservoir, indicating a low energy depositional environment. Facies observations from AS-4, AS-10 and AS-9 cores show merely bioclastic facies with a domination of coral, algae, and large foraminifera and mollusk fragments indicate a shallow marine, back-reef depositional setting. Furthermore, milliolids fossils and pyrite nodules appear in some intervals indicating well developed lagoonal and possibly restricted depositional system in this area. To date, none of existing cores record a massive boundstone facies which possibly would indicate a patch reef/reef development in this region, nonetheless the coral fragments are found widespread in all cores in varies extents and suggests the possibility that it might be develop somewhere between wells.

Different depositional facies are observed in AS-2 core showing grainier facies and high dolomite content. The lower part of the sequence is composed of detrital dolostone facies (breccias), while the upper section is composed of mainly packstone-grainstone facies. The dolostone breccia exhibits dolostone fragments with very poor sorting and the angular grain shape indicates rapid deposition, possibly debris flow. Similar facies also found in the lowermost part of the AS-5 and AS-7 wells (SWC thin section samples) support the interpretation that this sequence representing the rip-up sequence in earlier stages of the carbonate system. Appearance of small benthic forams mixed with planktic forams both in the lower and upper core section suggests a fore reef depositional environment (probably slope).

Strong indications of meteoric diagenesis is identified in all wells, but the most obvious was found in AS-9 and AS-10. Rubble core sample and high degree of chalkiness indicate the fresh water diagenesis impact on reservoir. Copious wispy dissolution seams, well developed moldic porosity and a number of oxidized layers are pronounced in these wells. However, it is important to noted that the cored section in AS-9 and AS-10 came from different depth intervals indicating that there are possibly multiple sub-aerial diagenesis controls in the reservoir.

Log analysis and core data display a non-linear relationship of porosity versus permeability versus depth ([Figure 4](#)) which is rather unusual in a single meteoric diagenesis model. Some porosity development is identified in deeper zones and indicate a more complex (possibly multiple), rather than single sub-aerial exposure/meteoric diagenesis. The internal seismic character of AS-3D data also suggest several carbonate progradation events which support this multiple exposure hypothesis ([Figure 5](#)).

Geological Model

Seismic Interpretation

A total of 128.26 km² 3D seismic data was used to image the size and geometry of Alur Siwah Field. Alur Siwah 3D seismic data is Pre-Stack Time Migration data that reduces uncertainties in textural attributes and seismic inversion interpretation. Well seismic ties have been done for five wells. Synthetic seismograms were generated using extraction of seismic data. The extracted wavelets are approximately a zero phase wavelet with small shift and length that vary between wells. Bulk-shifting, stretch-squeeze and iteration process of wavelet extraction process were only done for AS-8, AS-5 and AS-7, the other two wells, AS-9 and AS-10, have a good tie without performing changes to time depth data ([Figure 6](#)).

Structural seismic interpretation has been done for Top Peutu Limestone and Tampur Dolomite (Base Peutu Limestone). Top Peutu structure was picked as a strong peak that is the same as synthetic-seismic correlation in well seismic tie. Top Peutu is characterized in seismic as a base of on-lapping features of Lower Baong Sand. A number of faults were identified within Peutu intervals and the overlying section is also supported by variance attribute data. Based on the regional tectonic history and concept, the major tectonic regime that controlled the Alur Siwah faulting is strike-slip. This is expressed by a North-South fault with various vertical displacements that extended to the south, the Alur Kacang prospect, as a horse-tail of this dextral strike-slip fault. The major fault is located on the western side of Alur Siwah Field with an average throw of 200 ms. This major fault is interpreted as a strike-slip fault with western side as hanging wall in southern area and eastern side as hanging wall in the northern area. There are many other faults that are considered a byproduct due to strike-slip movement.

Internal zonation of seismic facies based on seismic character and relative impedance data were interpreted with support from the geological concept of Alur Siwah Peutu Limestone deposition. There are four zones of seismic pattern packages identified from seismic data which are defined as a result of higher order sea level rise that occurs during deposition of the Peutu Limestone interval. These zones were named as Cycle 1, Cycle 2, Cycle 3, Cycle 4 and Cycle 5 that possibly represent cyclical changes of sea level rise and falls that imprinted in the seismic data. Cycle 1 is interpreted to be formed during sea level rise of transgression. This package shows a series of onlapping features along the base of the Peutu Limestone. The distribution of this package is not widespread throughout the field. Cycle 2 is interpreted as a sediment package of regression when sea level rise and sediment supply increased. The distribution of this package is broader compared to the previous cycle and marked by downlapping features to the top of Cycle-1 package. Cycle-3 is interpreted as a continuation of regression and it is widespread throughout the field due to higher accommodation space with high sediment supplies. Cycle-4 and Cycle-5 are interpreted as an aggradational package and are locally distributed as a function of parallel amount between sediment supply and accommodation space. At this time, sea level started to rise so the carbonate tries to catch-up but due to rapid sea level rise or tilting of platform, carbonate development started to give up.

Variance and Ant-tracking attributes are used to help the structural interpretation. Using various parameters, several volumes of variance attributes were generated. These volume attributes show a consistent image of major faults across the Alur Siwah Field. These volume attributes were also used as an input for ant-tracking analysis. Extended interpretation of faults distribution using ant-tracking analysis has been done using several parameters of variance data as input for this process. Conditioning of data such as structural smoothing and filtering were

also performed before applying variance attribute. Ant-track result shows a major fault lineament and possible fracture intensity ([Figure 7](#)).

Seismic Inversion

In seismic inversion, PSTM 3D seismic data was used and has preserved amplitudes with low vertical seismic resolution and 28 Hz dominant frequency at the level of the Peutu Formation. This is due to the deep carbonate target at 9,100 ft subsurface. An average velocity in the carbonate of 13,123 ft/sec yields a vertical seismic resolution of approximately 115 feet.

The accuracy of the horizon interpretation of the carbonate is crucial for seismic inversion analysis. Picking the top carbonate and internal reflection character of the carbonate in conventional reflectivity data is difficult because of the chaotic and dimming seismic amplitude effects related to the low impedance of high porosity and facies changes in carbonates. To overcome this problem, a high frequency enhancement technique (Young and Wild, 2004), relative impedance inversion using a colored inversion method (Lancaster and Withcombe, 2000), and seismic inversion looping for validation of seismic interpretation were used.

More rigorous inversion was performed using the sparse spike approach, with a wavelet extracted from seismic data with well to seismic ties. A low frequency model was created by extrapolation of well impedance log data as a well-based model and integrated with Root Mean Square (RMS) seismic velocity and Low Frequency Model (LFM) from relative impedance to build initial model inversion approach to yield absolute impedance data. Inversion parameter analysis was tried in order to obtain the best parameter for running absolute acoustic impedance. The result shows good correlation, as a validation for the seismic inversion result.

Rock Properties Analysis

Cross-plotting acoustic impedance (AI) versus porosity from well logs shows that the gas and brine values are populated in overlap cluster, with a good relationship (minimal scatter). [Figure 8](#) shows a cross-plot analysis of acoustic-impedance versus gamma-ray and porosity using data from AS-2, AS-5, AS-7a, AS-8, AS-9, and AS-10, with color-key water saturation (S_w) and a hydrocarbon cut-off at 60%. Red represents gas in the carbonate reservoir and green represents brine. The cross-plot shows the hydrocarbon (gas) and brine carbonates still overlap based on AI value. So, the interpretation of AI cut off cannot be used to sharply separate a gas and brine in the carbonate reservoir. Cross-plot analysis of AI versus porosity in the carbonate reservoir shows a good linear relationship. This suggests that porosity can be estimated from AI by a transform equation. So, it is interpreted that low AI represents high-porosity, whereas high AI represents low-porosity carbonate. [Figure 9](#) shows cross-plot AI versus Porosity in carbonate reservoir, based on 5 zonation in Peutu Formation. [Figure 10](#) shows absolute AI section and map. The left panel shows AI inversion section through AS-7a and the second panel shows AI distribution map in zone-3 (example). AI sections can describe low AI (red to green) corresponding to high porosity distribution, while high AI (blue to dark blue) corresponds to medium and low porosity distribution.

The inversion results shown high porosity correlate with low acoustic impedance and low porosity is the opposite. The final map and cross section provide more realistic predicted effective porosity distribution geologically and help in understanding the subsurface image. As a result

of using updated reservoir modeling based on the seismic inversion, the field development plan can be revised to include the drilling of development wells.

Petrophysical Analysis

Only 7 of 10 wells are used for petrophysical analysis. Some of the available log data are derived from digitizing the print log. [Figure 11](#) shows the available log data and logs used for rock typing. There are 4 conventional cores (AS-2, AS-4, AS-9, AS-10) and 3 side wall cores (AS-7A, AS-8, AS-9) available. Depth matching between core and log is done using the relationship between core GR and log, correlation between porosity/permeability estimation trend and porosity/permeability from laboratory tests, and correlation between lithology from conventional core and log responses. Vsh is calculated from GR, density-neutron and/or sonic, depending on availability of data. Linear Vsh function is used in this study and minimum value of Vsh is chosen from each Vsh log analysis as the final result. The result of Vsh log is calibrated with grain size prediction which came from the core description and FMI log data that differentiate shale and non-shale qualitatively. The Alur Siwah Field has a tight reservoir as clearly seen from density and neutron response of logs. From log analysis the average effective porosity is 11% (average of porosity core is 11.27 %); porosity is calculated from neutron-density or sonic. There is no significant difference between effective and total porosity due to insignificant amount of shale content in this field. Results between log analysis and production tests show that porosity is relatively matched with test results. Water saturation is calculated using the Symondoux equation using parameters from SCAL DATA (AS-9 and AS-10); a (1), n (1.83) and m (1.91). The average of water saturation effective is 26%.

Production Logging Tool (PLT) data shows that the lower section of perforation-1 is the highest contributor on well test (38-42%), next is the upper section of perforation-1 (26-29%), perforation-2 (18-27%) and finally perforation-3 (3-17%). These values raise the possibility of having multiple layers of good quality reservoir which possibly relate to multiple episodes of sub-aerial exposure ([Figure 12](#)).

Rock type determination is guided by depositional and diagenesis information based on core and thin section descriptions. Data from AS-2, AS-7, AS-9, and AS-10 was used to derive six rock types, which are: (1) Fore Reef-Vadose, (2) Back Reef-Vadose, (3) Back Reef-Fresh Water Phreatic, (4) Lagoon-Vadose, (5) Lagoon-Fresh Water Phreatic, and (6) Back Reef-Dolomitized ([Figure 13](#)).

3D Model

Integration of all data mention above is used to define the relationship between well and seismic data prior to building a 3D geological model. For fault modeling, the input is from structural interpretation that has been validated by some attribute analysis (variance and ant-tracking). A rotation angle of 23.2 degree was used in pillar gridding to reduce the amount of truncated cells. To accommodate geological features clearly seen in seismic (progradation, retrogradation, aggradation), following the top was used to build the appropriate layering in each zone. The reference surface generated from thickness maps in each zone was also used as a control of the layering process. Truncated Gaussian Simulation (TGS) was used for linking the spatial relationship in this model. This method generated a trend probability map as an approach to model the facies depositional environment. Main input for spatial relationship is internal zonation that was interpreted from seismic 3D. As mention above, there are 5 zones in the Peutu Limestone which are acceptable by using the TGS. The porosity log and AI cube were used to generate the porosity model. The up-scaled porosity log was the main input in distributing the porosity because of its high resolution, while the

AI cube was treated as secondary input in distributing the porosity. Coefficient correlation from the cross-plot between Acoustic Impedance (AI) versus porosity was used to validate the porosity model ([Figure 14](#)). Then permeability was mapped using the formula of poro-perm transform for each facies generated by cross-plotting porosity versus permeability from core data. After thorough petrophysical analysis, water saturation was mapped ([Figure 15](#)) from the formula derived from the J function and normalized water saturation. With all the parameters having been distributed, the Original-Gas-In-Place was calculated. Formation volume factor, derived from laboratory measurements, is about 0.958 RB/MSCF. From the calculation, the estimate of OGIP is 406 BCF.

Conclusions

From the core analysis, no massive boundstone facies are identified from the Lower Miocene carbonate of the Peutu Formation. The fact that the coral fragments are found widespread in all cored sections leaves the possibility that it might be developed somewhere in this field. Multiple layers of good porosity identified in at least two different stratigraphic intervals suggest that multiple sub-aerial exposures influence the development of reservoir properties in the Alur Siwah Field. Integration of all available data has been done in building the geological model of this field. Relationship between core, logs, seismic, and production test data are being quantified to decode the complexity of the geological model.

Significant uncertainties still remain due to the percentage of data availability compare to the field size, especially in defining the facies model comprehensively. Uncertainty analysis should be done to increase the confidence level of building the geological model itself, which be used for developing this field.

Acknowledgements

We gratefully acknowledge Medco E&P Indonesia for supporting and permitting publication of this article, and our management and colleagues for their support, input, suggestions, and discussion. Numerous technical discussions with Alexis Carillat were instrumental to our understanding of the Peutu Limestone core descriptions and fault system in Alur Siwah. We would also like to thank SKKMIGAS and MIGAS for permission to publish this work.

References Cited

Bahar, A., and M. Kelkar, 2000, Journey From Well Logs/Cores to Integrated Geological and Petrophysical Properties Simulation: A Methodology and Application: SPE Reservoir Evaluation and Engineering, v. 3/5.

Barliana, A., G. Burgon, and C.A. Caughey, 1999, Changing Perceptions of a Carbonate Gas Reservoir: Alur Siwah Field, Aceh Timur, Sumatra: Indonesian Petroleum Association, Twenty Seventh Annual Convention Proceedings, IPA99-G-160.

Caughey, C.A., and T. Wahyudi, 1993, Gas Reservoir in the Lower Miocene Peutu Formation, Aceh Timur, Sumatra: Indonesian Petroleum Association, Twenty Second Annual Convention Proceedings, p. 191-218.

Lancaster, A., and D. Whitcombe, 2000, Fast-track 'Colored' Inversion: SEG 2000 Meeting Expanded Abstracts, 19, p. 1572.



Figure 1. Location of Alur Siwah Field.

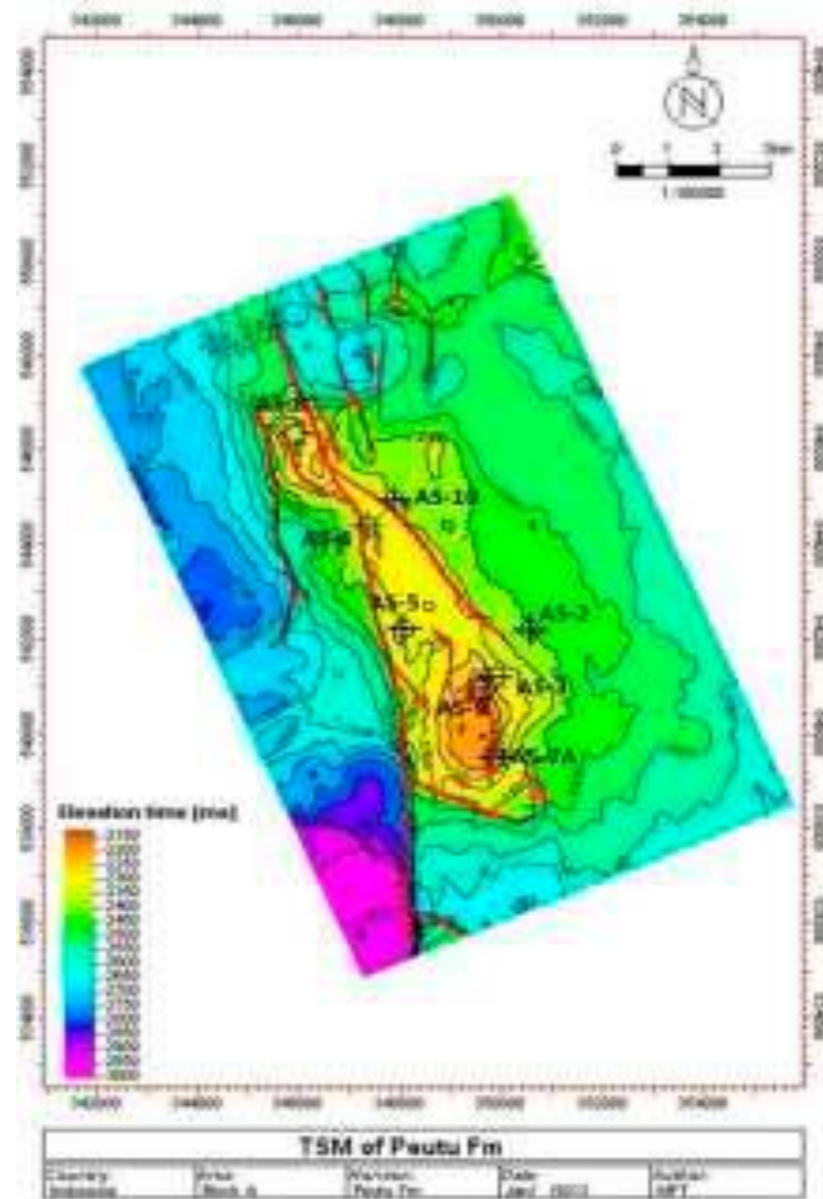


Figure 2. Time structure map of Peutu Limestone.

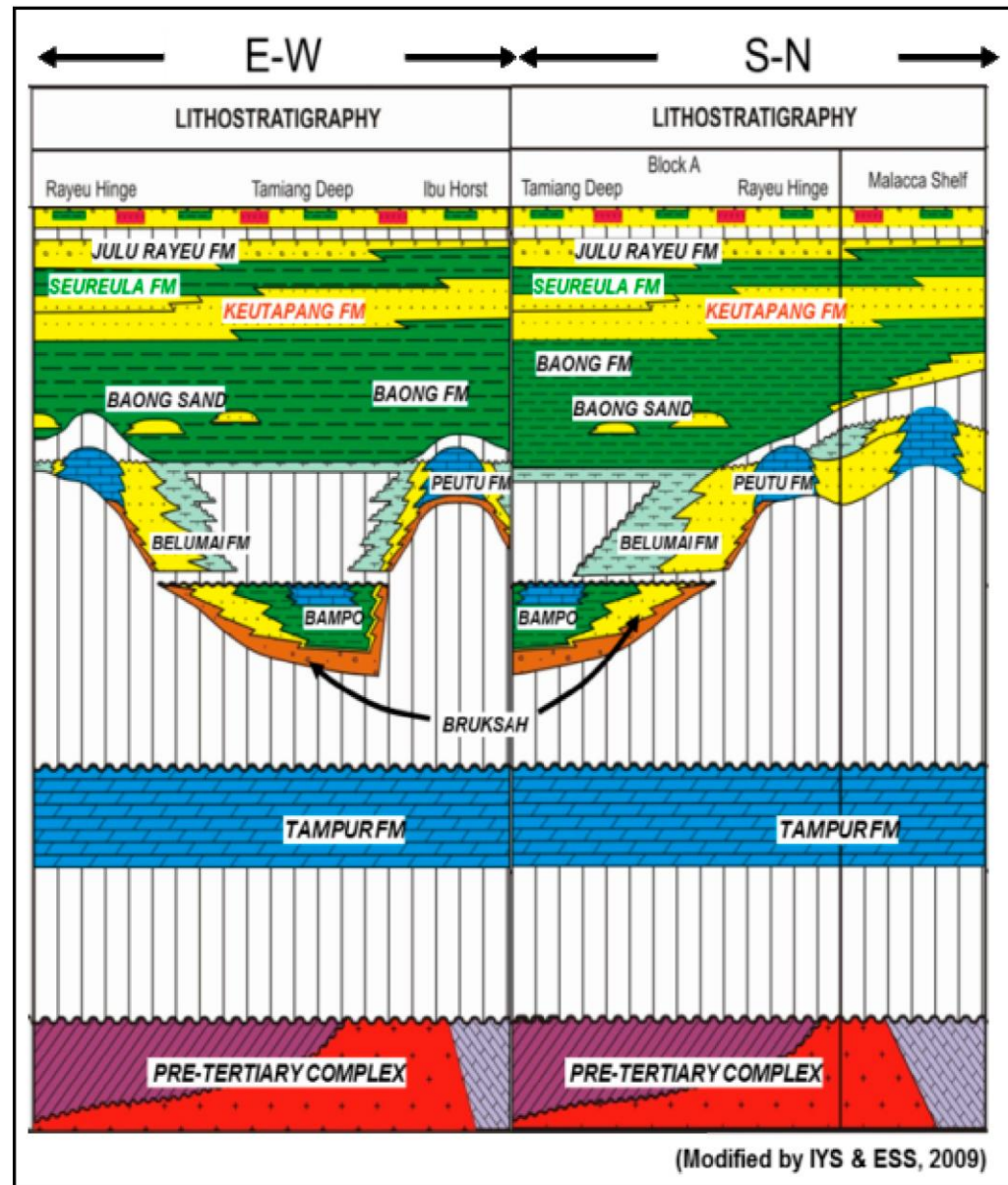


Figure 3. Regional stratigraphy of North Sumatra Basin.

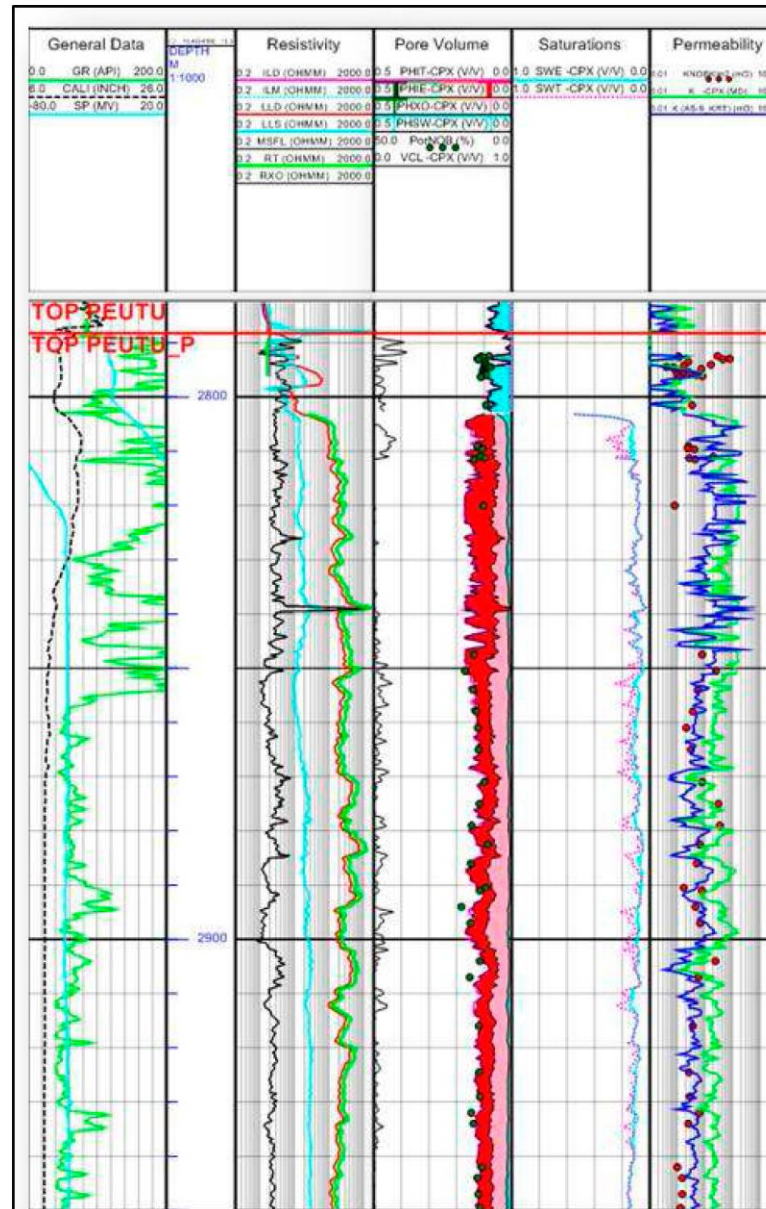


Figure 4. Non-linear relationship of porosity versus permeability versus depth.

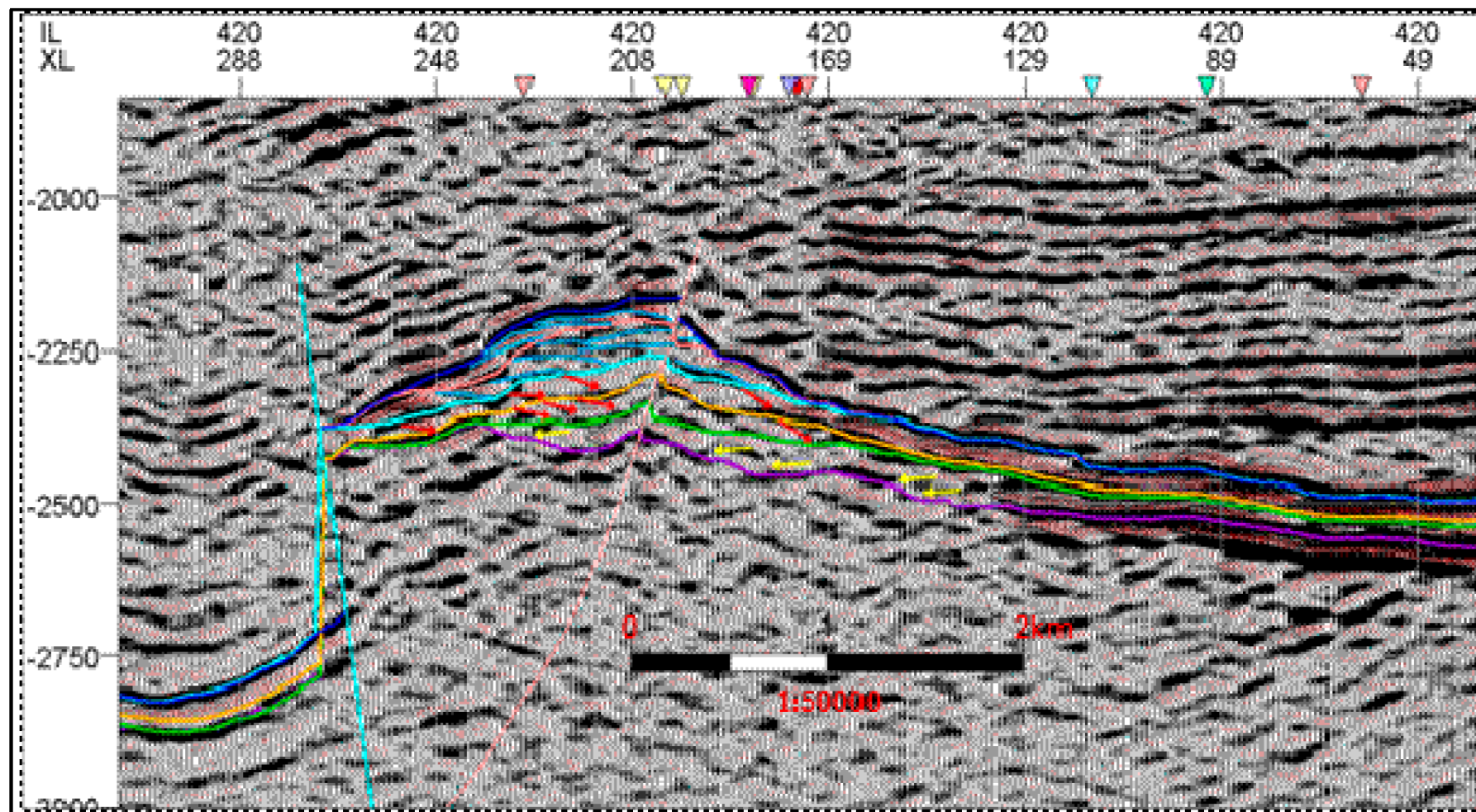


Figure 5. Seismic section shows internal seismic character that is interpreted as a product of depositional cycle.

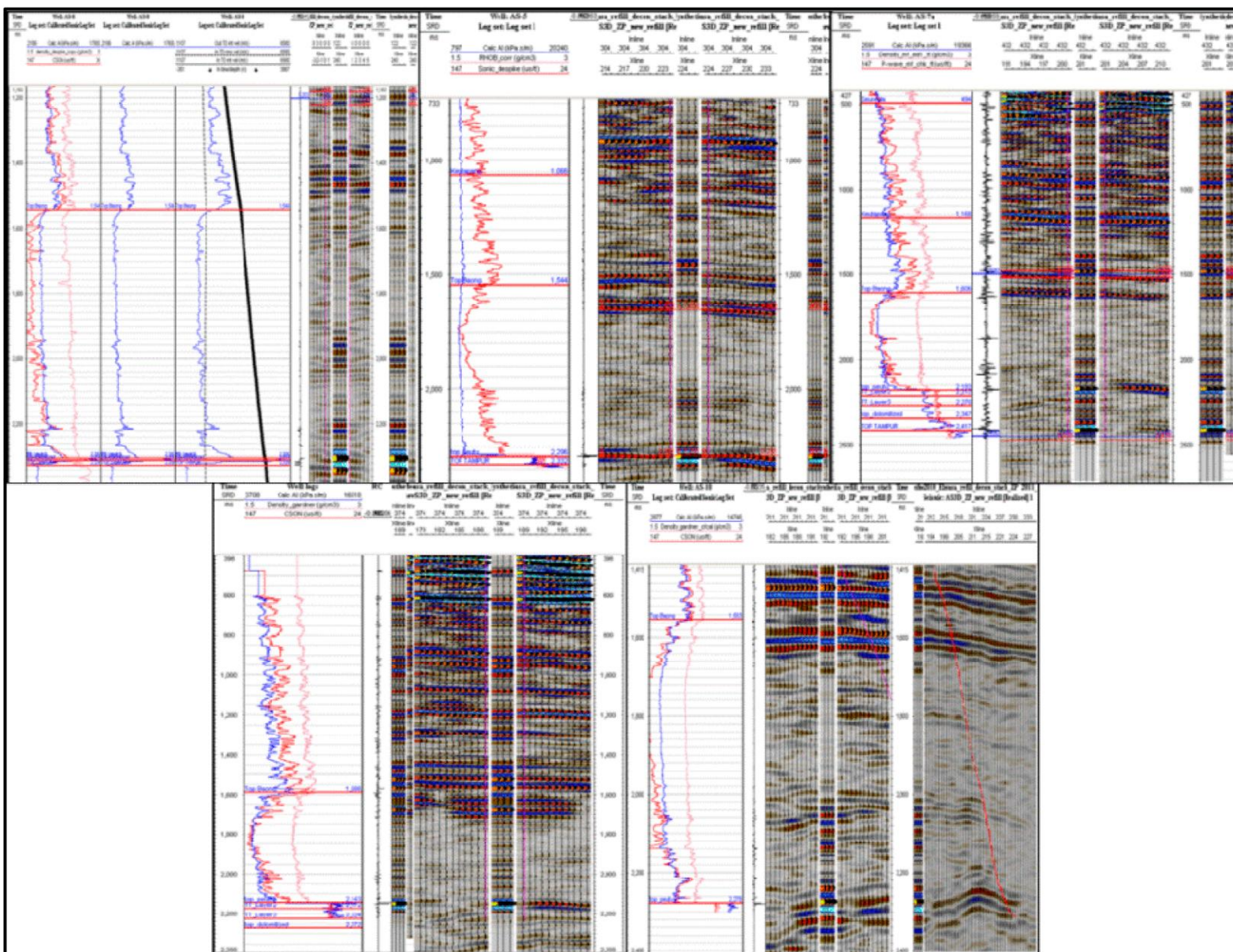


Figure 6. Well Seismic Tie of AS-8, AS-5, AS-7A, AS-9, and AS-10

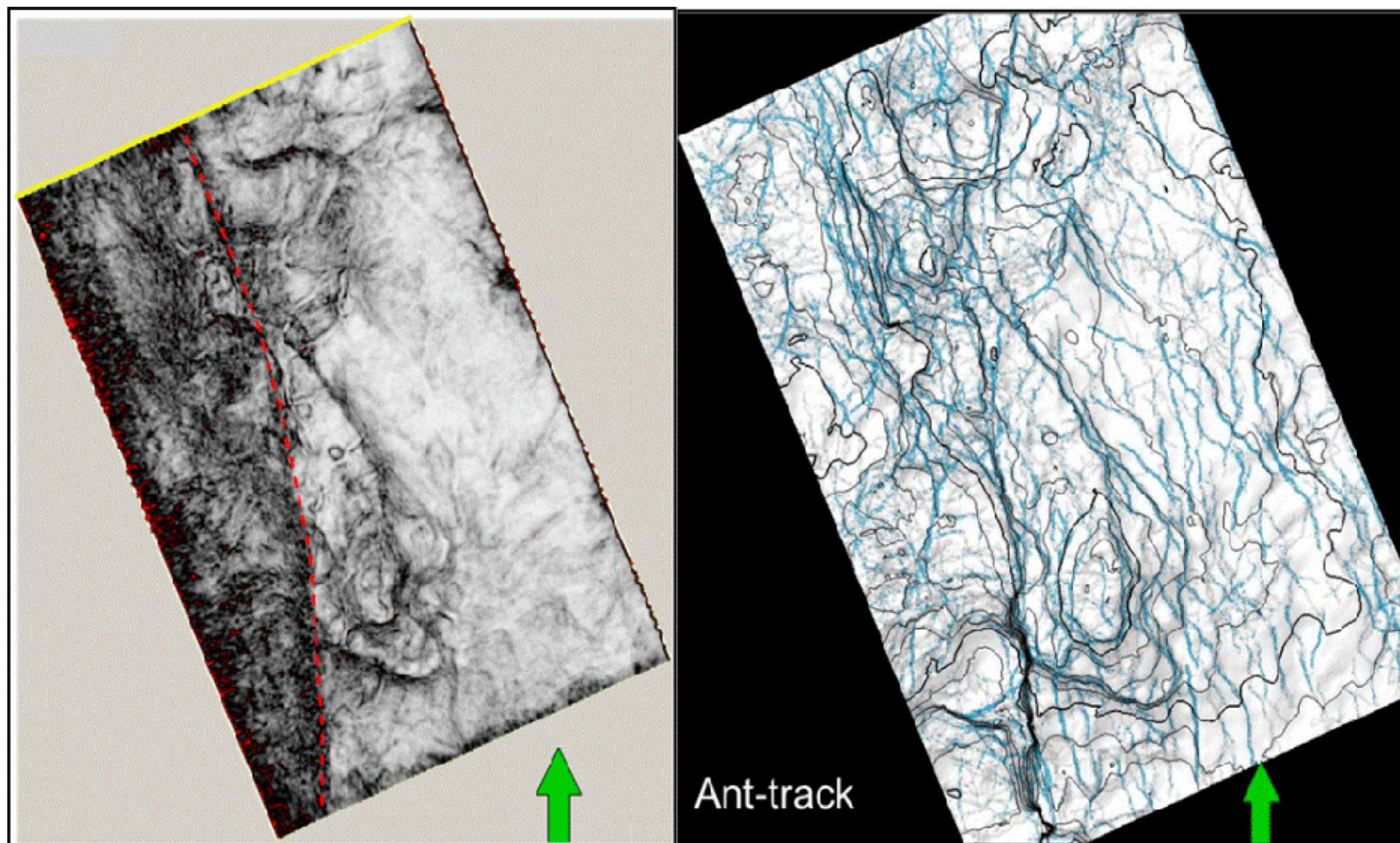


Figure 7. Variance and ant-track map shows a lineament of major faults and other faults in Alur Siwah.

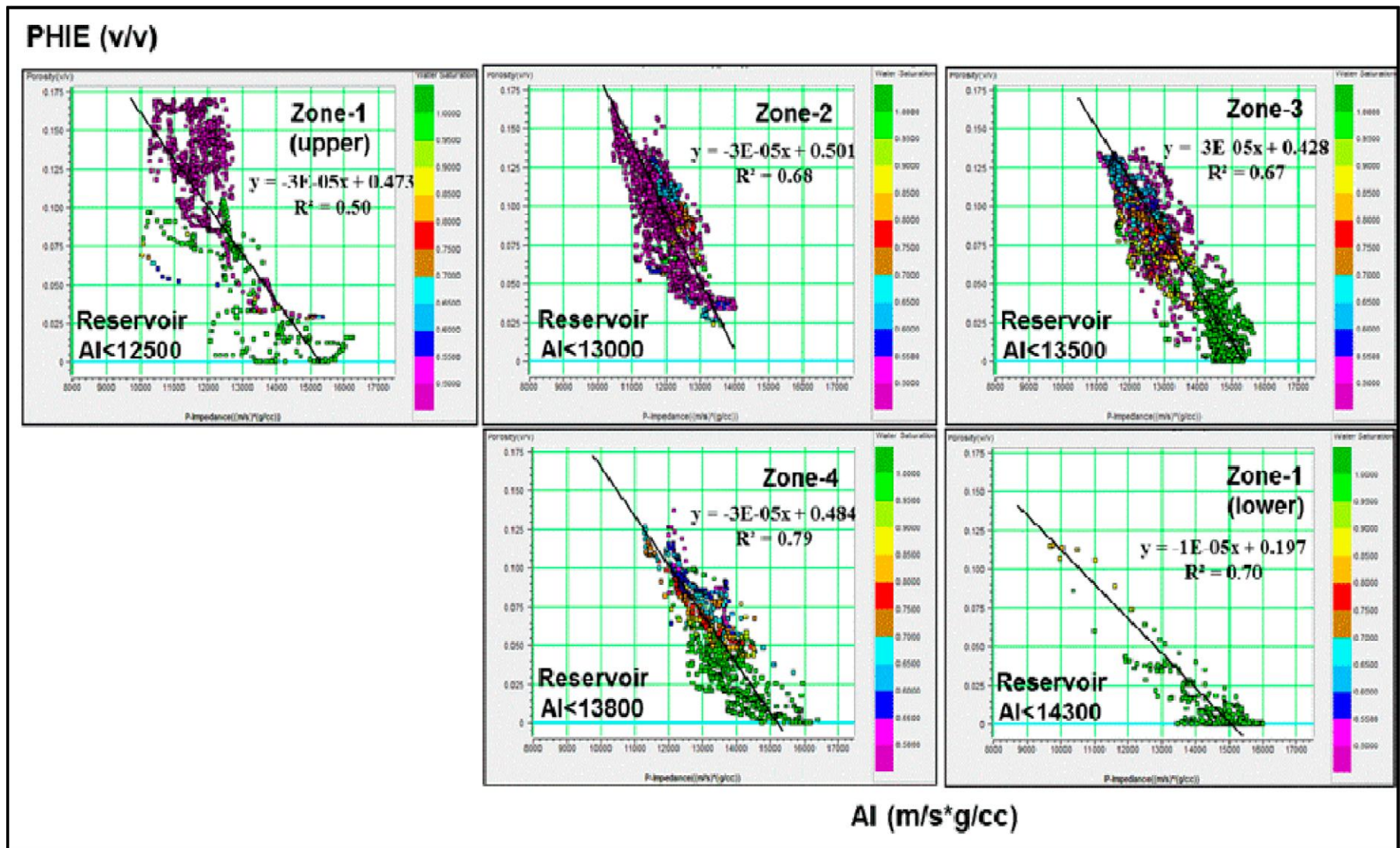


Figure 8. Cross-plot AI versus Porosity in carbonate reservoir with color key water saturation based on 5 zonation in Peutu Formation.

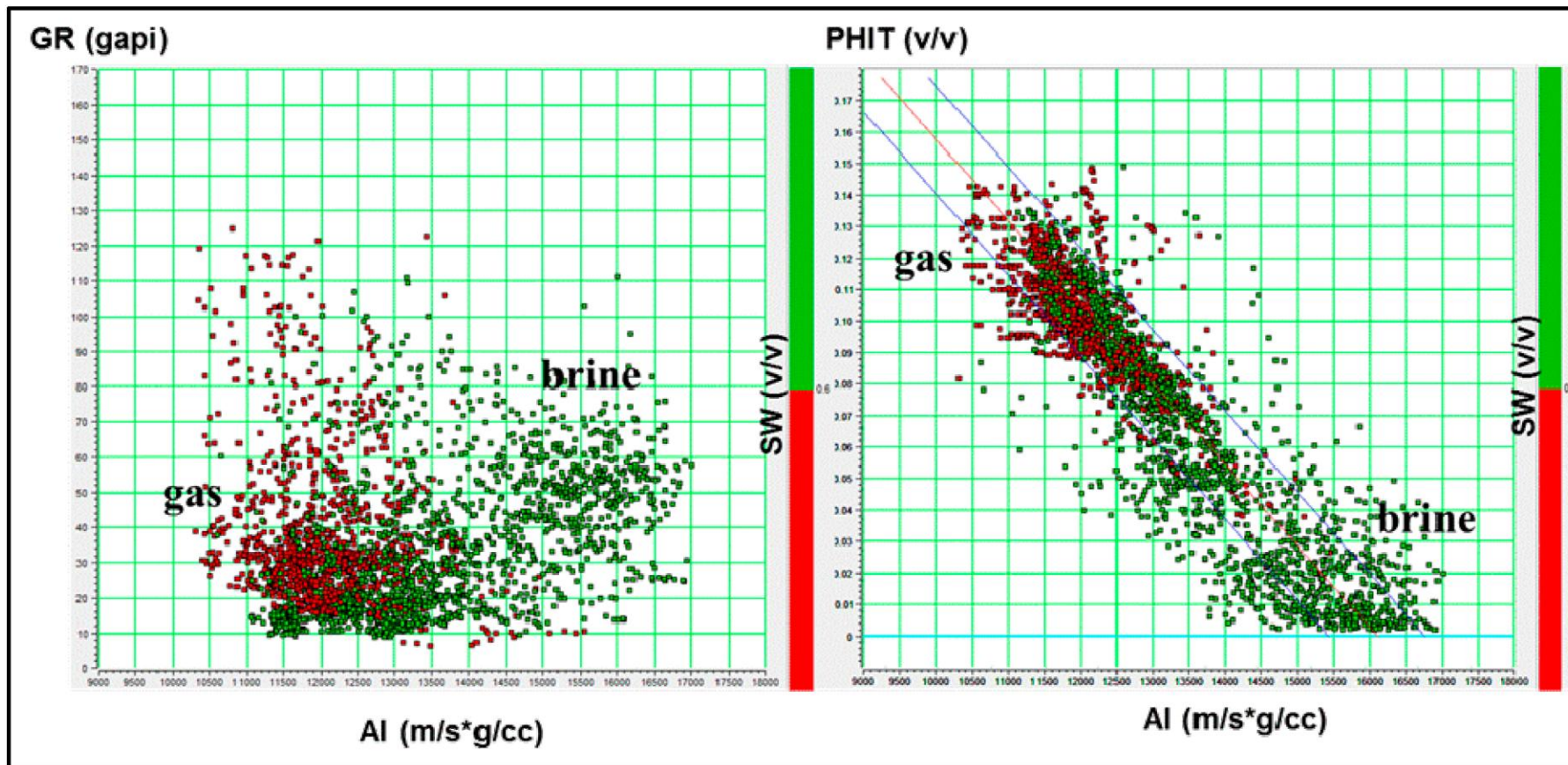


Figure 9. Cross-plot from wells AS-2, 5, 7a, 8, 9 and AS-10 in Peutu Formation with water saturation color-key (HC cut-off at 60%). Left panel shows AI vs. GR cross-plot; gas effect. Right panel shows AI vs. Total Porosity.

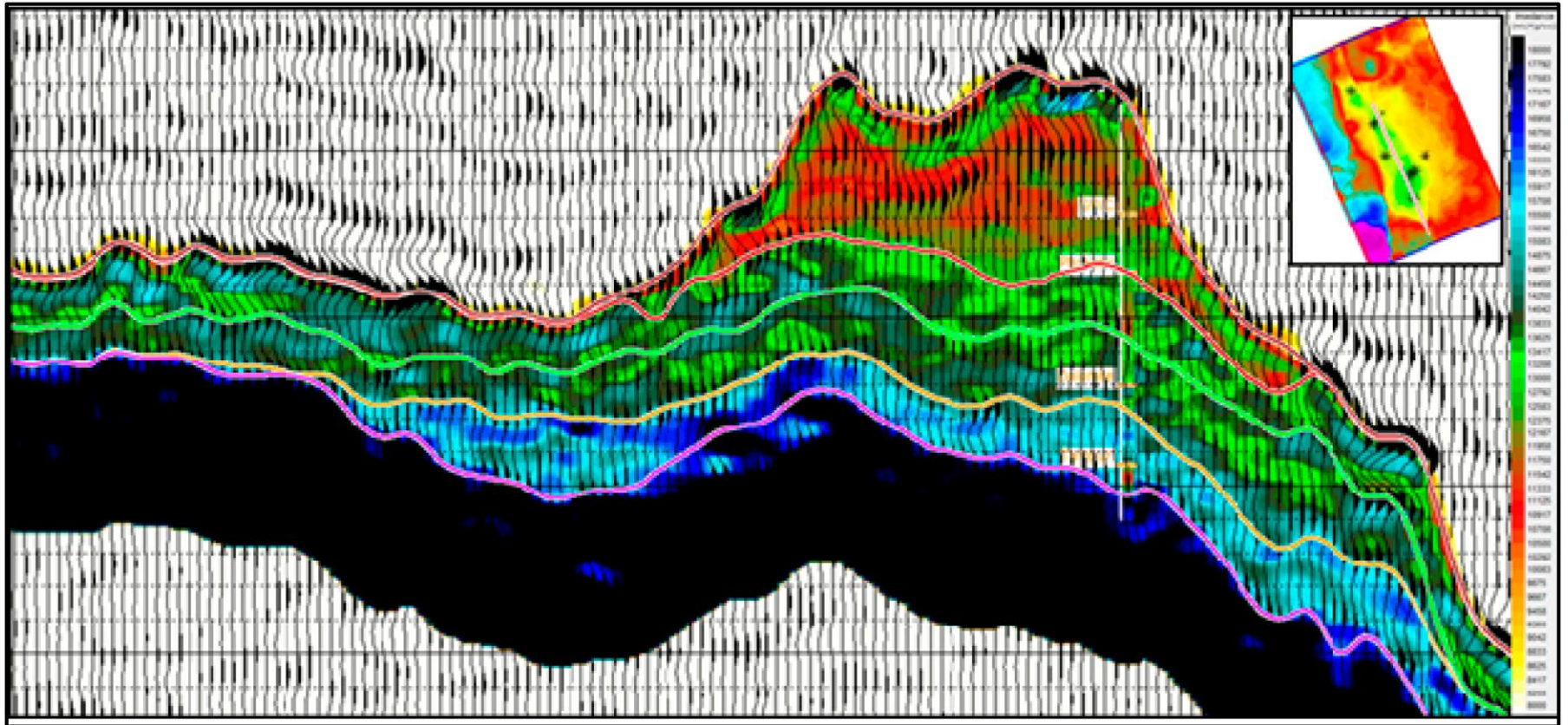


Figure 10. Absolute AI section shows AI inversion section through AS-7a.

Well Name	GR	SP	ILD	LLD	SN	LLS	MSFL	DT	RHOB	NPHI	PEF	CALI	DRHO	POTA	THOR	URAN
AS-2																
AS-3																
AS-5																
AS-7																
AS-8																
AS-9																
AS-10 ST																

Figure 11. Available logs of Peutu Fm in Alur Siwah Field, green marks available data, light red marks available data for rock typing.

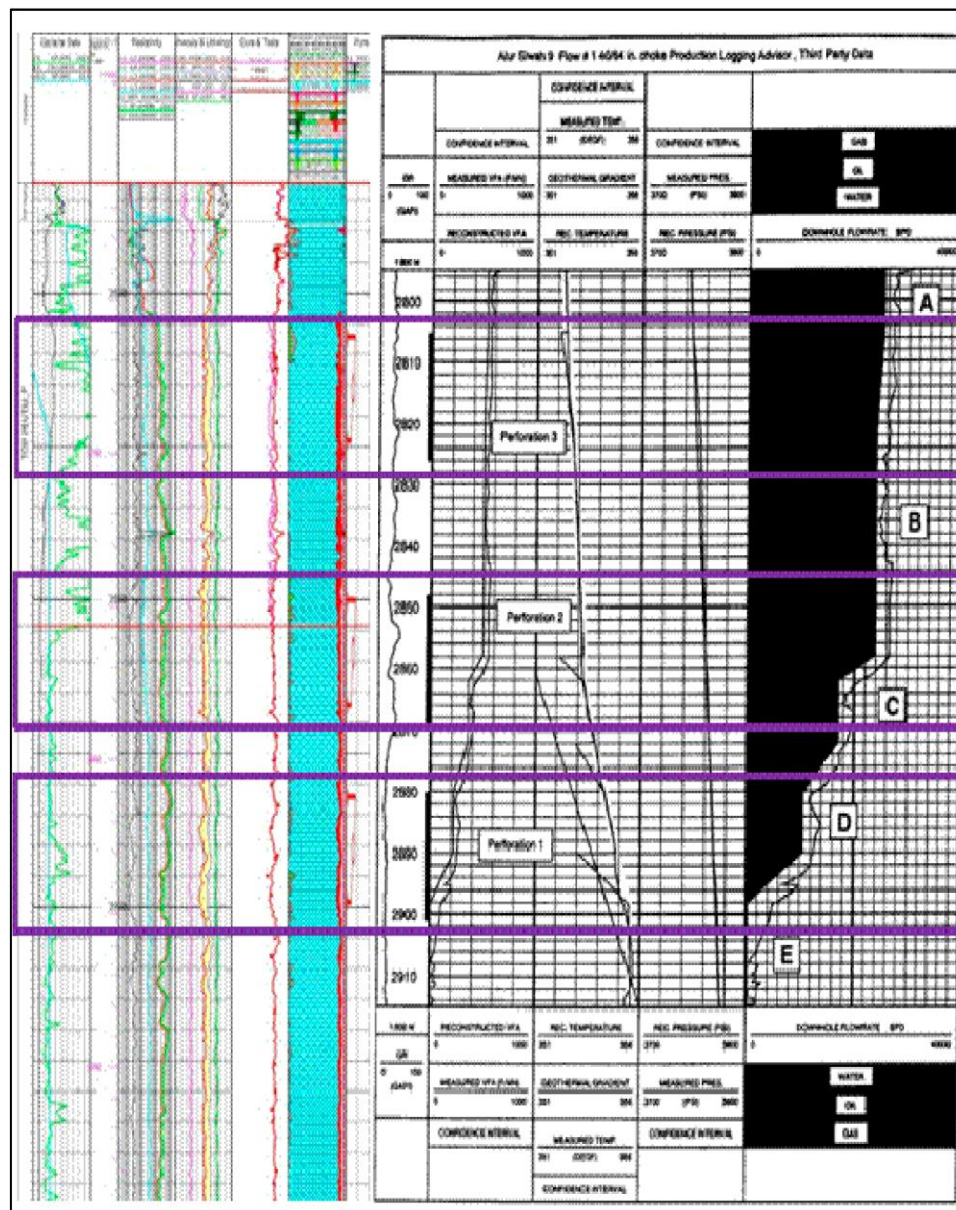


Figure 12. Comparison between log analysis and PLT data of AS-09 to prove multi-layered porosity development concept.

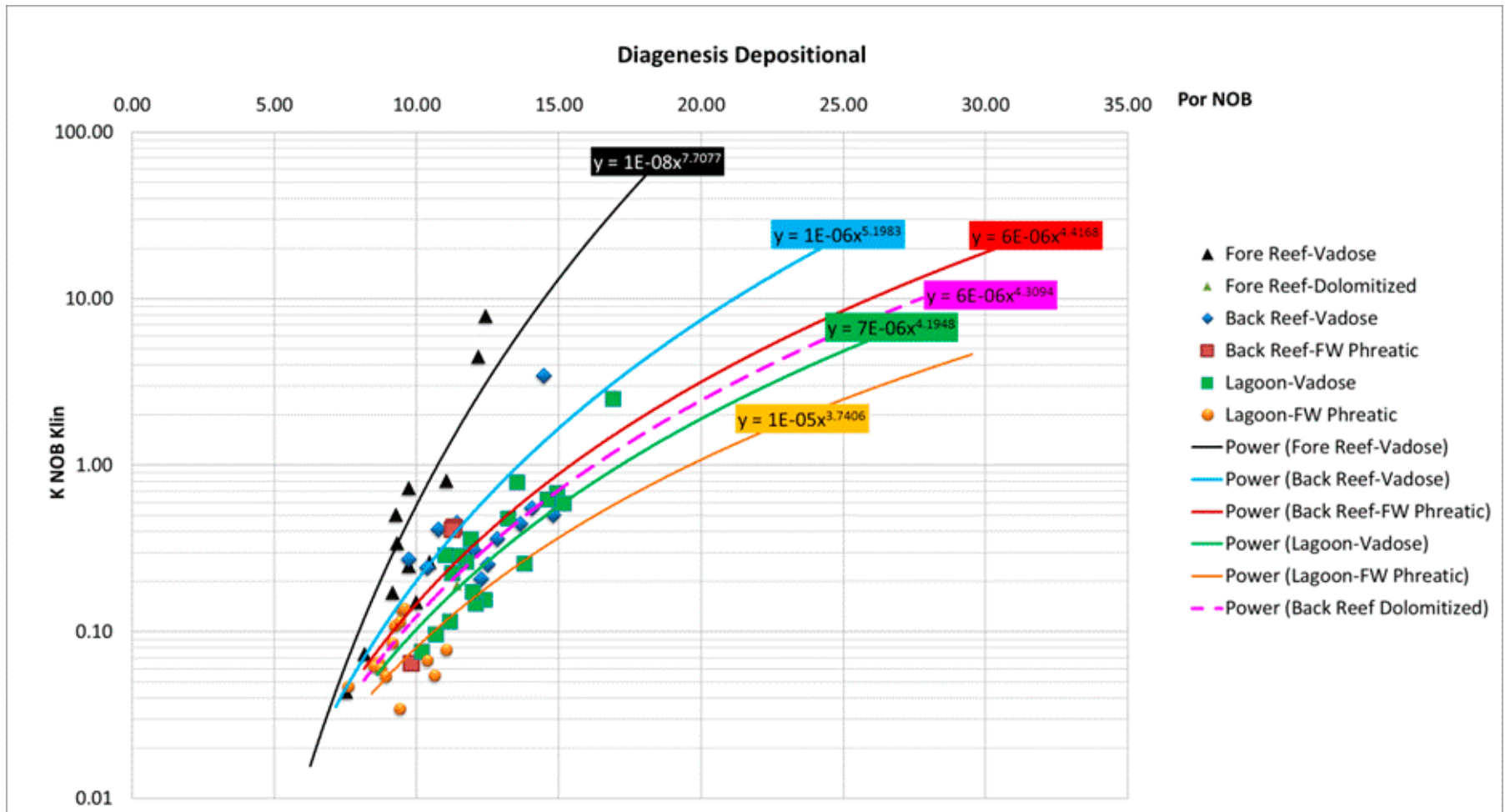


Figure 13. Relationship between porosity and permeability based on each rock typing based on core data.

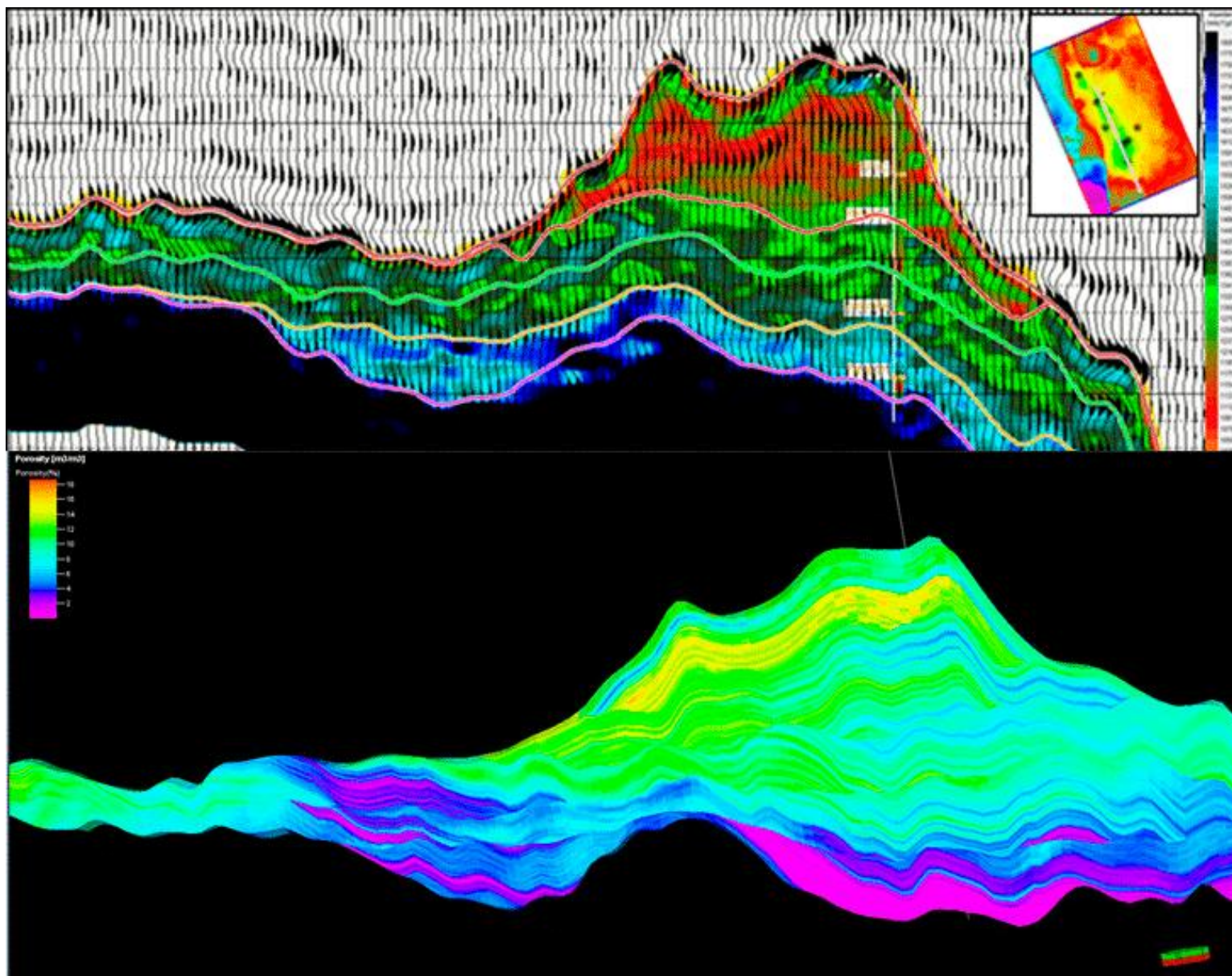


Figure 14. Coefficient correlation from the cross-plot between Acoustic Impedance (AI) versus porosity was used to validate the porosity model.

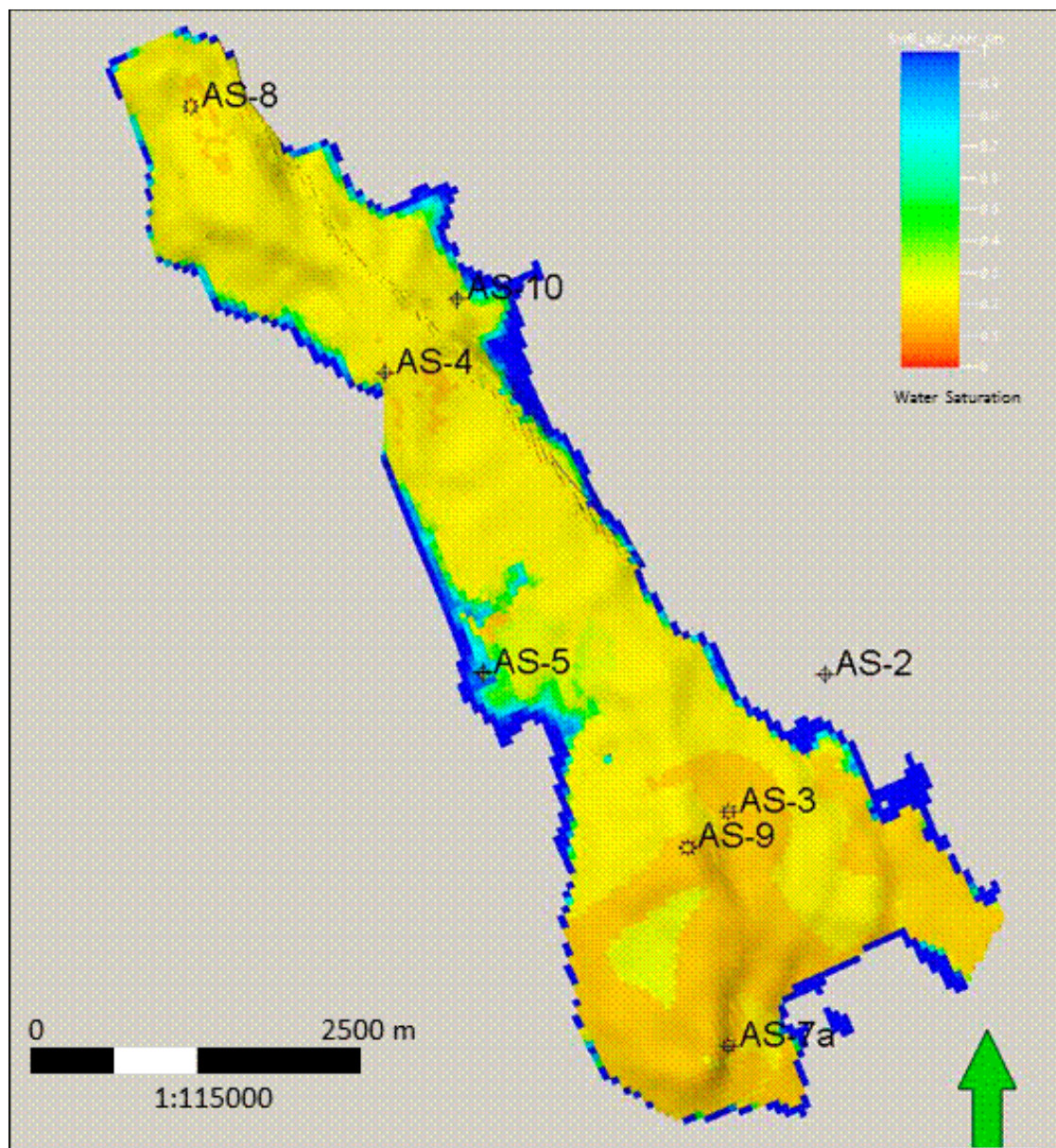


Figure 15. Water Saturation Model map.